J. Fluid Mech. (1988), *vol.* 186, *pp.* 539–558
Printed in Great Britain

Gravity waves on a rough bottom: experimental evidence of one-dimensional localization

By MAX BELZONS, ELISABETH GUAZZELLI AND OLIVIER PARODI

Département de Physique des Systèmes Désordonnés, UA 857 du CNRS, Université de Provence, Centre de Saint-Jérome, F-13397 Marseille CEDEX 13, France

(Received 4 March 1987)

We present experimental evidence of the localization of linear gravity waves on a rough (i.e. random) bottom in a one-dimensional channel. The localization phenomenon is observed through very precise measurements in a wave tank. Viscous dissipation and rough-bed finite-size effects are examined. The experimental estimation of the localization lengths are compared with the theoretical predictions of Devillard, Dunlop & Souillard (1988). Finally, the resonant modes due to the disorder are directly observed for the first time.

1. Introduction

The interaction of surface gravity waves with a rough bottom is a subject of fundamental importance to coastal engineers and sedimentologists. Some pre-existing topography may provide a mechanism for coastal protection and for possible dune growth if the bed is erodible. More precisely, submerged parallel bars may reflect incident waves, the combination of incident and reflected waves leading to a partially standing wave structure with all that this implies for preferred regions of deposition and erosion on the sand bed. Davies (1982*a*, *b*) has demonstrated that reflected waves can be resonated by equally spaced bars if the bar wavelength is one-half that of the incident waves. Experiments demonstrating this resonant reflection have been reported by Heathershaw (1982) and Davies & Heathershaw (1984). This kind of resonant reflection is known as Bragg reflection in solid-state physics. It also corresponds to the first forbidden band found by Brillouin in the quantum theory of solids: a beam of electrons with energy in the forbidden range is totally reflected by a regular lattice, which is modelled as a periodic variation in the potential field (see Kittel 1983).

Prior to those of Davies there exist papers on long waves over periodic bottoms (McGoldrick 1968; Rhines 1970; Rhines & Bretherton 1973) and, more recently, some other authors motivated by his work have considered the resonant-interaction phenomenon (Mitra & Greenberg 1984; Mei 1985; Dalrymple & Kirby 1986; Kirby 1986). Although the correspondence with solid-state physics has been pointed out in some of these works, none of them considers the crucial modification which happens in the case of a random bottom. It has been suggested by Guazzelli, Guyon & Souillard (1983) that the phenomenon known as Anderson localization in solid-state physics should be observed for shallow gravity waves if the bed is random.

The theory of localization deals with linear waves, described by a Schrödinger equation, a Helmoltz equation or a similar wave equation, propagating in a static disordered medium. The waves undergo many partial reflections and transmissions

from the scattering centres in the disordered medium and the various transmitted and reflected waves, which have random dephasing, interfere with each other. The theory of localization predicts the behaviour resulting from all these interferences. The basic result is that, if the disorder is strong enough, the wave will not propagate in the medium. More precisely, the stationary solutions or proper modes are exponentially localized, i.e. they decay exponentially along the medium with a rate of decay called the localization length (see Thouless 1974, 1982; Lee & Ramakrishnan 1985; Souillard 1987). In a one-dimensional medium, any disorder is strong enough to induce the exponential localization phenomenon (see for instance Borland 1963; Ishii 1973; Delyon, Lévy & Souillard 1985). The localization phenomenon was initially discovered in the study of electric conductivity of disordered solids. Since the localization phenomenon is not specific to electrons but is a genuine wave-interference effect, several applications of localization ideas have been proposed for classical waves propagating in one-dimensional disordered media: acoustic waves (Hodges 1982; Hodges & Woodhouse 1983; Baluni & Willemsen 1985; Dépollier, Kergomard & Laloe 1986; Kirkpatrick 1985), electromagnetic waves in plasmas (Escande & Souillard 1984), third or fourth sound waves in helium liquids (Cohen & Machta 1985; Condat & Kirkpatrick 1986), light waves (Bouchaud & Daoud 1986; Flesia, Johnston & Kunz 1987), electrical waves in a chain of random impedances (Akkermans & Maynard 1984).

The present study follows the preliminary work of Guazzelli *et al.* (1983) which was one of the first attempts to study localization on a macroscopic scale. The principle of an experiment to demonstrate the localization phenomenon was described and some estimations of the localization length were derived for the simplest case examined, namely linear shallow-water theory. The present paper deals with the interaction of linear gravity waves with a static one-dimensional random bottom and gives experimental evidence of the localization phenomenon. Parallel to the present work, theoretical calculations have been performed by Devillard, Dunlop & Souillard (1987) for the same kind of bottom as used in the experiments in order to enable comparisons between measured and predicted localization lengths.

Localization theory should apply to the simplest model of shallow-water gravity waves, i.e. the linear long-wave equation (the drastic physical limitations of which are discussed by, for example, Whitham 1974):

$$\eta_{tt}(x,t) = g(H(x)\,\eta_x(x,t))_x, \tag{1}$$

where g is the acceleration due to gravity, the horizontal x-axis is taken at the mean free-surface level ($y = 0$), $\eta(x,t)$ is the vertical displacement of the free surface and $y = -H(x)$ defines the bed, which only varies in the x-direction. For this simple model it should be possible to demonstrate the close analogy with solid-state physics.

The corresponding stationary equation for waves of frequency $f = \omega/2\pi$ is

$$-\omega^2\eta(x) = g(H(x)\,\eta_x(x))_x. \tag{2}$$

In the case of a horizontal flat bottom $H(x) = H_0$, the stationary solutions are plane waves with velocity $(gH_0)^{\frac{1}{2}}$. In the case of a sinusoidal bottom, (2) could be transformed into a Mathieu equation with forbidden bands corresponding to strong reflection of the incident wave appearing at $2k/K = 1, 2, 3, 4, \ldots$ where k is the wavenumber of the waves and K that of the bottom.

In the case of random bottom, (2) is quite similar the stationary Schrödinger equation with a random potential. The localization length $\xi(\omega)$ for a frequency ω can

be computed from the Lyapunov exponent γ through $\xi(\omega) = \gamma^{-1}(\omega)$. The Lyapunov exponent is given from the asymptotic behaviour of the solution of the stationary equation (2). For a bottom comprising steps with random heights and lengths, Devillard *et al.* (1987) have computed this exponent from a product of random transfer matrices. The resulting localization length diverges for small frequencies as ω^{-2}. Since the long-wave approximation is no longer valid for large frequencies, calculations have been made on the basis of linear potential theory using the renormalized transfer matrix introduced by Miles (1967). The predictions of the potential theory follow closely those of the long-wave theory for small frequencies. The resulting localization length diverges both at small and large frequencies. The numerical results show a range of frequencies where the localization length is close to its minimum value and might be observable in a realistic experiment.

However, there are certain physical limitations of linear potential theory which have been discussed by Devillard *et al.* (1988) and which may be stated as a set of simple conditions:

$$\eta k, \frac{\eta}{H}, \quad \eta k^{-2} H^{-3} \ll 1. \tag{3}$$

Moreover, the effect of surface tension is neglected in linear theory. It is necessary also to take into account dissipation and finite-size effects which are outside the scope of the original theoretical study and which are the two principal experimental limitations on the observations of the localization phenomenon. The localization length depends on frequency and disorder; localization could be inobservable if the localization length is too large, e.g. much larger than the natural dissipation length of the wave or the size of the system (i.e. the length of the rough bed). These two limitations are now discussed from an experimental point of view.

First, dissipation implies a damping of the wave; this attenuation has a different nature from that induced by localization, which is an interference phenomenon involving back-scattering of the wave. If the wave is damped over a very short lengthscale by viscous dissipation, the additional damping due to localization might not be observable. Since only very rough estimates of viscous dissipation can be made, we have assumed, with good experimental justification, that viscous damping of the wave amplitude is almost the same on a random bottom as on a periodic bottom with the same average characteristics. Thus, we have extracted a localization length characteristic of the damping due to the randomness of the bed in the range of frequencies where localization is visible. Experimental results for the random case are compared with those obtained for the periodic case throughout this study.

Secondly, in a realistic experiment, the random bottom has a finite length and, more precisely in our experiment, its length is of the same order as the localization length in the range of frequencies where localization is observable. This gives rise to fluctuations in the transmission coefficient (or the reflection coefficient) which are not present in very large systems such as those used in the numerical calculations of the localization lengths (Devillard *et al.* 1988). These fluctuations, well known in solid-state physics (see for example, Azbel 1983 and Lee & Ramakrishnam 1985), are due to the occurrence of resonances. The eigenmodes, which are exponentially localized for an infinite system, are turned into resonances for a finite system. Since these resonant modes are trapped along the random medium, the wave could pass by tunneling and thus the transmission will be enhanced for the corresponding resonant frequencies. This implies a sample-to-sample dependence of the transmission. Throughout this study, the two effects of dissipation and finite-size are examined.

In §2 the experimental set-up is described and in §3 the experimental results are

presented and compared with theoretical predictions. Finally, in §4, the results are discussed and the validity of the comparison with the theoretical model is examined.

Further details of these results may be found in Belzons *et al.* (1987) and Guazzelli (1986).

2. Experimental techniques

2.1. *The wave-tank and the beds of variable depths*

The experiments were carried out in a glass-walled wave tank (length = 4 m and width = 0.39 m), shown schematically in figure 1. The average water depth H_0 was varied between 1 and 4 cm. Water depths were determined to within an estimated 0.2 mm. A bottom composed of periodic or random steps was built into a false flat bottom with the mean water depth H_0. The different bottoms varied only in the x-direction along the tank so that, apart from weak edge effects, the motion of the wave was one-dimensional.

Three main bottoms were used to in the experiments (see figure 2). The first bottom R is a random one consisting of 58 steps. The heights and lengths of the steps are randomly chosen with uniform distribution respectively in $H_0 \pm \Delta H$ and $L_0 \pm \Delta L$ with $H_0 = 1.25$ cm, $\Delta L = 2.0$ cm and $L_0 = 4.1$ cm. This bottom corresponds to the 58 first steps of the theoretical bottom R_{th} composed of 10000 steps used in the numerical calculations of the localization length by Devillard *et al.* (1987). Table 1 gives the precise geometry of the random bottom R for 58 heights H' and lengths L. We have also constructed other random bottoms by different permutations of the random steps.

The second bottom P is periodic and corresponds to the mean characteristics of the random one, i.e. the length of the steps is L_0, the heights of the steps are successively $H_0 \pm \sigma_H$ where $\sigma_H = 0.75$ cm is the standard deviation of the previous random heights and, finally, the two bottoms have the same total length. The wavelength of P is $\Lambda = 8.2$ cm.

The third bottom RS is a randomly spaced one, i.e. only the lengths of the lower steps of the bottom P are randomly chosen with uniform distribution between $L_1 = 2.0$ cm and $L_2 = 8.0$ cm. Diminishing the mean depth of water increases the amplitude of the bottom modulation and thus of the disorder, which is characterized by $\Delta H/H_0$.

Other bottoms were used to perform auxilliary experiments to provide an experimental justification for the assumption concerning viscous dissipation outlined in §1, i.e. that this dissipation only depends on the average characteristics of the bottom. These bottoms were as follows (see figure 2):

a periodic bottom P′ consisting of the same higher steps as the bottom P, but of shorter lower steps. Its wavelength is $\Lambda = 2\pi/K = 6.2$ cm;

a periodic bottom P_1 consisting of steps with lengths $L_0 = 4.1$ cm. The heights of the higher steps are successively $H_0 + \Delta H_1$ and $H_0 + \Delta H_2$ with $\Delta H_1 = 0.5$ cm and $\Delta H_2 = 1.5$ cm. The heights of the lower steps are $H_0 - \Delta H_3$ with $\Delta H_3 = 1$ cm. The wavelengths of the two Fourier components of this bottom are $\Lambda_1 = 2\pi/K_1 = 8.2$ cm and $\Lambda_2 = 2\pi/K_2 = 16.4$ cm;

a periodic bottom P_1' which corresponds to the mean characteristics of the bottom P_1, i.e. the length of the steps is L_0 and their heights are successively $H_0 \pm \sigma_H$, where σ_H is the standard deviation of the heights of P_1. The total length of each of these different bottoms is the same as that of the bottom P.

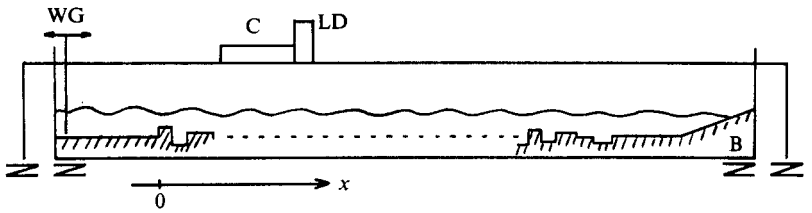

FIGURE 1. Schematic diagram of the wave tank showing the positions of the wave generator WG, the absorbing beach B, the carriage C and the linear detector LD in relation to the random bed.

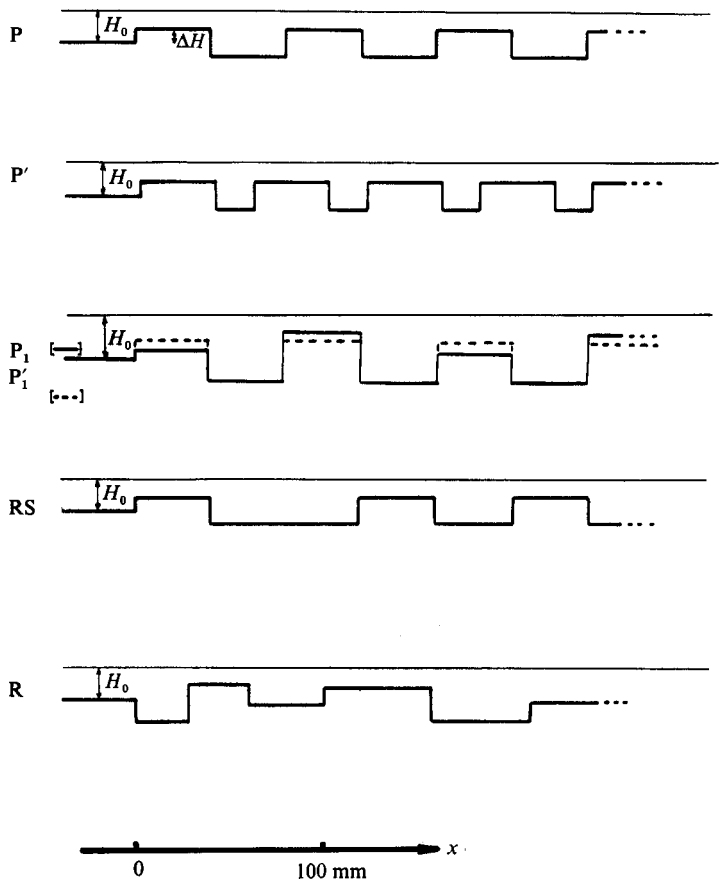

FIGURE 2. Schematic diagram of the variable bottoms used in the experiments.

At the end of the tank, a 12° slope rubberized-fibre wave-absorbing beach B was built to prevent waves from being back-reflected onto the variable bottom. The length of the beach was equal to the wavelength of the longest-period waves at the highest water level examined. Shorter-period waves were expected to be more readily absorbed by the beach than these long-period waves. We discuss back-reflection by the beach in §3.1. This effect has been examined in detail by Davies & Heathershaw (1984).

N	H' (mm)	L (mm)	N	H' (mm)	L (mm)	N	H' (mm)	L (mm)
1	−12.00	27.00	11	2.50	57.00	21	4.00	39.50
2	8.50	32.00	12	9.50	38.00	22	12.00	45.00
3	−3.50	41.00	13	4.00	24.50	23	9.00	52.50
4	6.00	58.00	14	2.00	47.50	24	−11.00	24.50
5	−11.50	52.00	15	4.50	24.00	25	−5.50	48.00
6	−1.50	36.50	16	−3.50	43.00	26	2.50	41.50
7	1.50	41.00	17	11.00	50.00	27	5.58	43.50
8	−9.00	32.50	18	−12.50	37.00	28	−11.00	22.50
9	0.50	46.50	19	1.50	34.00	29	6.50	33.50
10	12.00	24.00	20	−4.50	50.00	30	7.00	53.50
31	9.00	20.50	41	−4.00	49.00	51	−10.50	48.00
32	−7.00	27.50	42	−8.50	52.50	52	−2.50	29.00
33	−10.00	22.50	43	−4.00	52.00	53	6.00	36.00
34	−1.00	35.50	44	4.50	34.50	54	7.00	29.50
35	−8.00	45.50	45	11.00	44.00	55	−4.50	56.50
36	−8.00	41.50	46	−9.00	41.00	56	−4.00	29.00
37	−4.50	35.00	47	5.00	58.50	57	−10.00	56.50
38	−9.00	49.50	48	11.50	40.50	58	−6.00	47.50
39	11.00	36.50	49	−2.50	53.00			
40	9.00	49.00	50	−5.50	38.00			

TABLE 1. Heights H' and lengths L of the 58 steps of the random bottom R. The heights H' are the heights above (+ sign) or under (− sign) the mean level H_0. N is the number of the step.

2.2. *The wave generator*

Monochromatic sinusoidal waves of amplitude $A_i(x)$ were generated using a piston-type wave generator WG:

$$\eta_i(x,t) = A_i(x)\cos(kx-\omega t). \tag{4}$$

The vertical paddle of the wave generator was driven by a microstepping motor, and the motor monitored by an Apple IIe microcomputer. The wave frequency $f=\omega/2\pi$ ranged between 1 and 5 Hz with bulkhead amplitudes $\leqslant 1$ mm. The frequency was determined to an accuracy better than 0.0001 Hz. The wave generator was at all times operated within these limits to ensure that the waves were linear gravity waves. We shall discuss this point in §4.

Since the time taken for the wave system to attain a steady state was always shorter than the duration of the experimental runs, the measurements described in §3 were representative equilibrium conditions.

2.3. *The wave measurements*

Measurements of the wave elevation were made using an optical method which is more accurate than the usual wave gauges (resistance or capacity type). This method has been developed by Hebrard & Toulouse (1983) at the Toulouse ONERA-CERT. A laser beam (a 5 mW He–Ne laser) is incident at a right angle on the free water surface (see figure 3). The diffusion spot is focused on a linear detector LD (a 256 pixels linear camera), using a lens L. The displacement $A'B'$ of the image spot follows linearly the surface wave elevation AB.

In order to avoid volume diffusion, the water was coloured with blue ink. On the other hand, to ensure a good surface diffusion, a small quantity of soluble oil (0.05%)

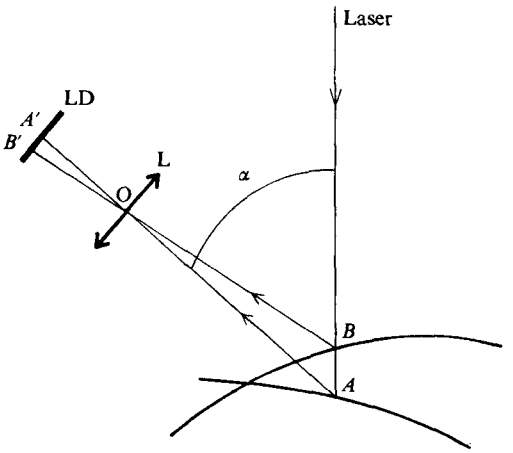

FIGURE 3. Sketch of the optical set-up used in the measurement of the wave elevation.

was added to the water. The resulting kinematic viscosity of the liquid was only 3% higher than that of pure water.

The reading of the linear detector was controlled by the Apple IIe microcomputer which was synchronized with the wave generator to permit data acquisition over several (typically 20) wave periods. From records of the wave elevation $\eta(x,t)$ obtained at position x along the tank, the wave amplitude $A(x)$ was obtained at each position from the relation

$$\eta(x,t) = A(x)\cos(\omega t + \phi(x)), \tag{5}$$

where $\phi(x)$ is the phase of the wave (the reference phase being given by that of the wavemaker).

To check the linearity of the wave, we examined the wave elevation more precisely by fitting it to the relation

$$\eta(x,t) = \sum_n A_n(x)\cos(n\omega t + \phi_n(x)), \tag{6}$$

thus obtaining the amplitudes $A_n(x)$ and phases $\phi_n(x)$ of the fundamental wave and its harmonics.

All the optical devices and the linear detector LD were mounted on a carriage C (see figure 1) which could be slid along the top of the tank on two rails. The motion of the carriage was driven by a stepping motor which itself was monitored by the microcomputer. The smallest available displacement corresponding to one step was 0.0456 mm. Thus wave amplitudes were measured all along the tank, the use of stepping motors for the motions of both the wave generator and the carriage ensuring reproducibility of the measurements.

With this experimental set-up it has been possible to determine, for any given frequency, the reflection coefficient R, which is defined as the quotient of the reflected and incident wave amplitudes. The interference of the reflected and incident waves induces a modulation of the resulting wave amplitude $A(x)$ which varies between $A_{\max} \sim 1+R$ and $A_{\min} \sim 1-R$. From the measurement of $A(x)$ on the up-wave side of the variable-bottom region, we have deduced the rate of stationary waves $\mathrm{RSW} = A_{\max}/A_{\min} = (1+R)/(1-R)$ and thus the reflection coefficient R. Measurements have been made at distances greater than half a surface wavelength

from the start of the variable-bottom region in order to reduce the effect of the evanescent waves generated by the rough bottom.

Wave amplitudes have also been measured throughout the variable-bottom region and thus the damping length l of the wave has been deduced by fitting $A(x)$ to the relation

$$A(x) \sim \exp\left(\frac{-x}{l}\right). \tag{7}$$

We have used a least-squares fit of $\ln A(x)$ to x; in the examples given below in figures 9 and 10, the correlation coefficient lay between 0.85 and 0.95.

3. Experimental results

As already mentioned in §1, the more drastic of the two experimental limitations on the observation of the localization phenomenon is due to the effect of viscosity. Viscous dissipation results in an exponential damping of the waves over the bottom for laminar boundary-layer flow, such that their amplitude behaves roughly as

$$A(x) \sim \exp\left(\frac{-x}{d}\right), \tag{8}$$

where d is a characteristic length called the dissipation length. The assumption of laminar flow is justified except on the sharp corners of the steps, since the wave Reynolds number in the present experiments was always very small: on a flat region $Re = U^2/\omega\nu \sim 100$, where ν is the kinematic viscosity and U the local velocity amplitude in the potential-flow region outside the thin wave boundary layer.

We know that in order to observe localization, the length d must not be too small with respect to the localization length ξ; otherwise the additional damping due to disorder would not be experimentally measurable. However, even if the effects of viscosity are weak, which is the case for water, it does not seem *a priori* easy to separate the effect of disorder, characterized by ξ, and the effect of viscosity, characterized by d, from the total experimental damping length l.

Dissipation is due not only to the friction on the bottom and sidewalls of the channel but also to the generation of vortices at the edge of each step and, therefore, seems quite impossible to calculate. Thus we have been constrained to make only a rough experimental estimation of the viscous dissipation using the assumption presented in §1. A set of auxiliary experiments on periodic beds has been carried out to support this assumption.

As a general rule in what follows, the experimental results obtained for a random bed are discussed with reference to the associated periodic bed.

3.1. *Reflection coefficient*

Initially we compare experimental results for the random and associated periodic beds. For this comparison, the results are plotted on the same graphs (figures 4–6).

The periodic bottom P has been studied for two water depths: $H_0 = 3$ cm $< \Delta H/H_0 = 0.25$) and $H_0 = 1.75$ cm ($\Delta H/H_0 = 0.43$). In both cases the plot of R versus the wave frequency f shows (figures 4*a*, 5*a* and 6*a*) a strong maximum at a frequency such that the wavenumber k satisfies approximately the Bragg condition for a sinusoidal bed of wavenumber $K = 2\pi/\Lambda$, namely $k = \frac{1}{2}K$. For this reason, the frequency range around this maximum will be called the first forbidden band. For the smallest water depth $H_0 = 1.75$ cm (strongest modulation of the bed:

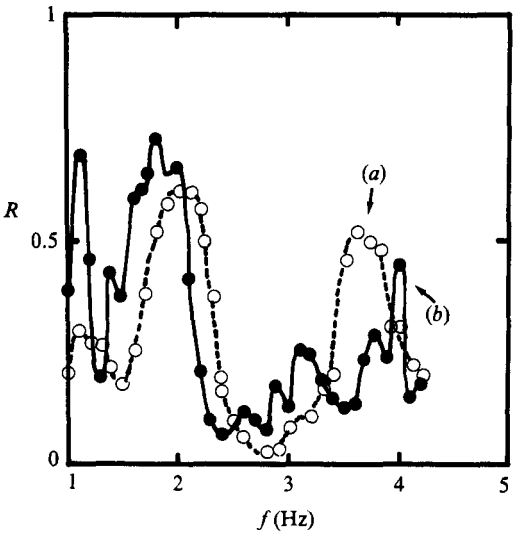

FIGURE 4. Results for the reflection coefficients of the bed P (curve *a*) and bed RS (curve *b*) with $H_0 = 1.75$ cm.

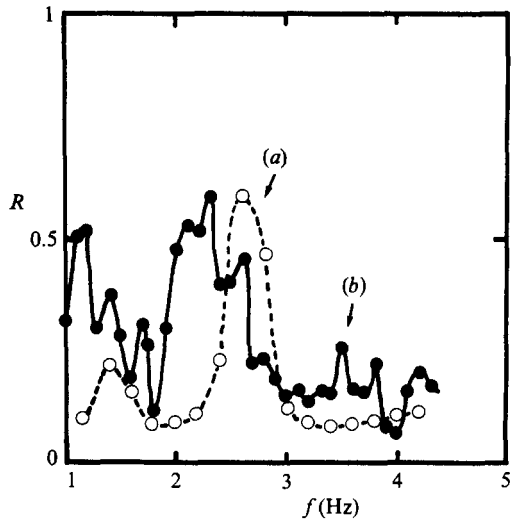

FIGURE 5. Results for the reflection coefficients of the bed P (curve *a*) and bed R (curve *b*) with $H_0 = 3$ cm.

$\Delta H/H_0 = 0.43$, see figure 4*a* or 6*a*), a second sharp peak of R appears in the investigated frequency range. This peak is the manifestation of a second forbidden band located about a frequency such that $k = K$.

Let us now examine the behaviour of R for random beds. The randomly spaced bed RS used with a water depth $H_0 = 1.75$ cm, i.e. a ratio $\Delta H/H_0 = 0.43$, is moderately disordered since, in the frequency range of interest, the product of the average wave number $\langle k \rangle$ with the standard deviation σ_L of the step lengths L is close to one: $\sigma_L \langle k \rangle \sim 1$. By comparison with the periodic case, we may observe from figure 4 that in the $R(f)$-spectrum which is chiefly modified in the passing bands, we can still recognize the first forbidden band.

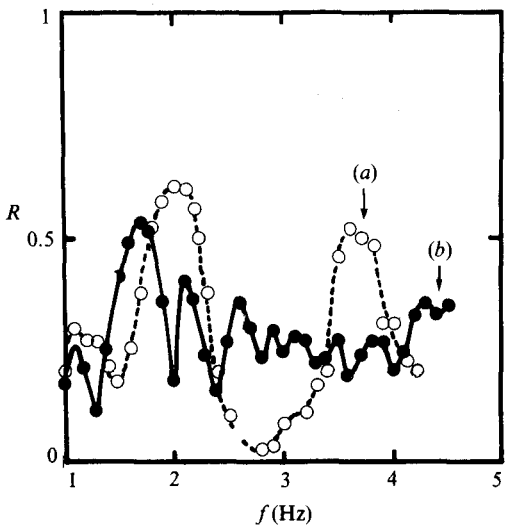

FIGURE 6. Results for the reflection coefficients of the bed P (curve *a*) and bed R (curve *b*) with $H_0 = 1.75$ cm.

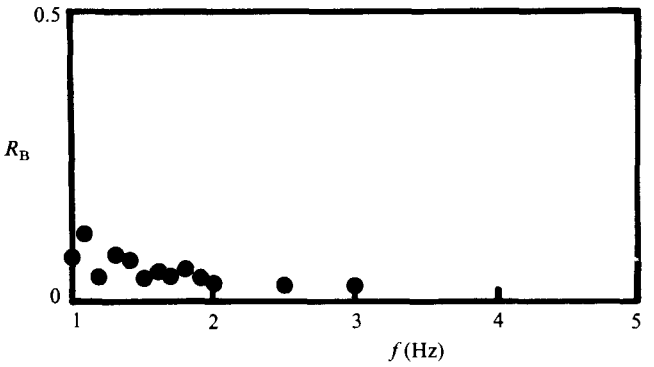

FIGURE 7. Results for the reflection coefficients of the beach with $H_0 = 1.75$ cm.

The bed R with both random step lengths and heights has been studied for two water depths: $H_0 = 3$ cm and $H_0 = 1.75$ cm so that the disorder has been varied with the ratio $\Delta H/H_0 = 0.42$ and 0.71. In the case of the smallest disorder ($H_0 = 3$ cm, $\Delta H/H_0 = 0.42$) we can still discern in the plot of $R(f)$ the outline of the first forbidden band of the periodic case (figure 5). On the other hand for the strongest disorder ($H_0 = 1.75$ cm, $\Delta H/H_0 = 0.71$) the spectrum of $R(f)$ is completely modified as compared with that for the periodic case: it displays huge oscillations over the entire frequency range and the passing bands have disappeared (figure 6).

Figures 7 and 8 show the reflection coefficients for the beach, for which wave measurements were made on a flat bottom at the same location of the wave tank as for the above experiments to ensure that the reflected waves should be damped by viscosity in the same way. The beach reflection coefficients are of the order of $R = 0.1$–0.2 below 2 Hz because the length of the absorbing beach is not long enough. Above 2 Hz the beach reflection is negligible. In the low-frequency range, the beach back-scattering introduces uncertainty into values of the reflection coefficient. Davies & Heathershaw (1983) have shown that the true reflection coefficient R_T is

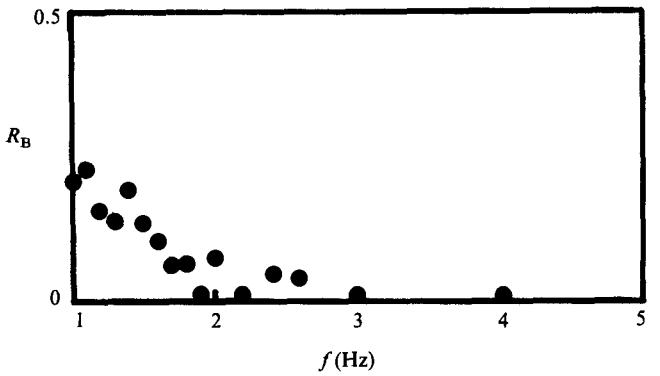

FIGURE 8. Results for the reflection coefficients of the beach with $H_0 = 3$ cm.

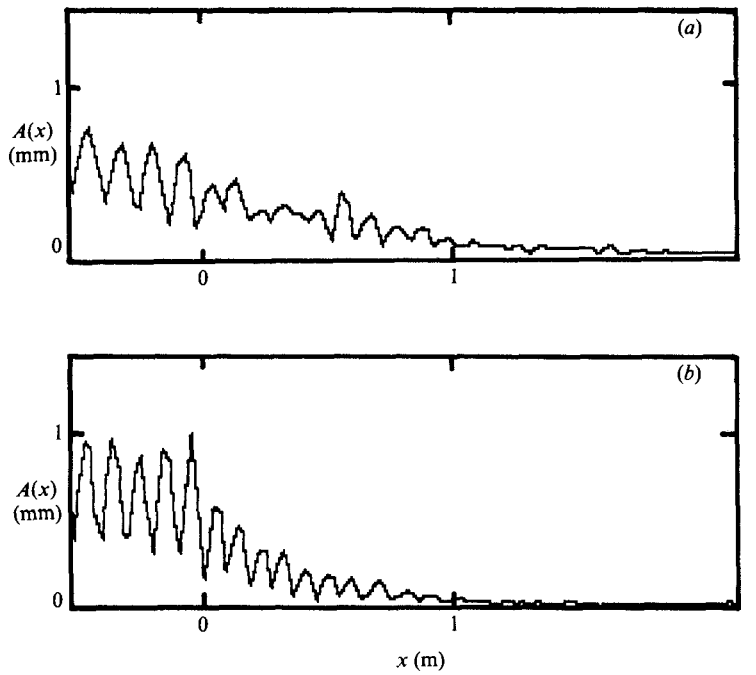

FIGURE 9. Variation of the amplitude of the wave elevation along the wave tank for the bed RS. Abscissa 0 corresponds to the beginning of RS. Curves (*a*) ($f = 1.6$ Hz) and (*b*) ($f = 1.9$ Hz) represent respectively a resonant and a non-resonant case.

estimated in the experiments to within a range of uncertainty around the measured value R given by $R_T = R \pm R_B$, where R_B is the measured reflection coefficient of the beach.

3.2. *Behaviour of the wave amplitude along the random bed*

Owing to the great accuracy of the experimental set-up the observed behaviour of $A(x)$ is strictly connected with the random character of the bed. For a given realization of the random bed, one can observe, at frequencies corresponding to oscillations in the $R(f)$-curve, quite clear reinforcements of $A(x)$ which are never observed for a periodic bed: at these frequencies, the wave does not decay monotonically along the random bottom but increases in its middle region (figures 9*a* and 10*a*).

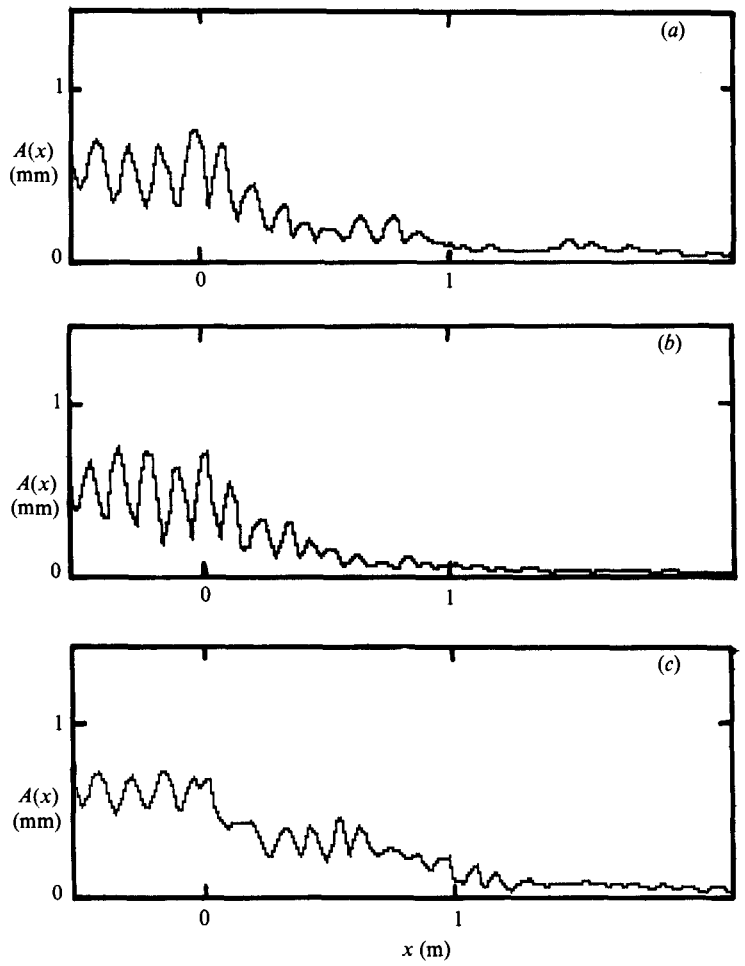

FIGURE 10. Variation of the amplitude of the wave elevation along the wave tank for the bed R. Abscissa 0 corresponds to the beginning of R. Curves (*a*) ($f = 1.5$ Hz) and (*b*) ($f = 1.7$ Hz) represent respectively a resonant and a non-resonant case for the same realization of the bottom. Curve (*c*) ($f = 1.5$ Hz) is obtained for another random realization of the bottom.

This behaviour is the manifestation of what has been described in the introduction as the resonant modes of the random bed. First, it has been checked experimentally that these resonances in the damping of $A(x)$ occur for frequencies corresponding to a decrease in the reflection coefficient. The wave can be better transmitted through the help of resonances located near the middle of the bottom (figure 10*a*). This explains the strong fluctuations observed in the $R(f)$-curves (figure 6*b*).

Secondly, the resonances are very sensitive to frequency variations for a given random bottom: figures 9(*a*) and 10(*a*) show these resonant modes for the RS and R beds respectively. In both cases, a small frequency variation makes them disappear (figures 9*b* and 10*b*). In addition, for two different resonant frequencies, the spatial locations of the corresponding resonances are different.

Thirdly, the occurrence of these resonant modes is sample dependent. Experiments on different random realizations of the bottom R obtained by permuting the random steps in a random way, show that, for a given frequency, the resonances strongly depend on the random realization (figure 10*a*, *c*).

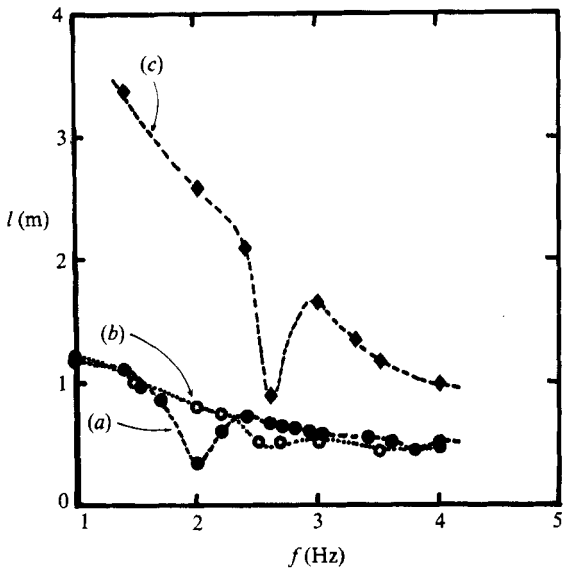

FIGURE 11. Results for the damping length l of the wave along the beds P (curve a) and P′ (curve b) with $H_0 = 1.75$ cm and the bed P (curve c) with $H_0 = 3$ cm.

3.3. *Estimation of the dissipation length*

The damping of the amplitude $A(x)$ of a wave propagating over a periodic bed is solely caused by viscous dissipation; hence the variation of $A(x)$ can be approximately fitted by (7) with $l = d$ out of the forbidden bands.

Figure 11 shows the behaviour of l versus frequency for the bed P with $H_0 = 3$ cm (figure 11c) and $H_0 = 1.75$ cm (figure 11a). On to the general variation of l are superimposed local depressions which mark the forbidden bands where the wave is almost totally reflected. The damping length decreases when the frequency or the parameter $\Delta H/H_0$ is increased.

In order to estimate the viscous dissipation length, we have performed auxillary experiments to characterize separately the influence of the step lengths and heights. It should be noted that the results concerning the two periodic beds P and P′, which differ only in their wavelength, show the same value of l out of the forbidden bands (figure 11a and b). The viscous attenuation length in the passing bands seems to depend essentially upon the water depth over the highest steps. The position of the forbidden bands depends upon the linear density of steps, whereas their depth and width are given by the detail of the profile.

We have carried out experiments first with the periodic beds P_1 and P_1' described in §2.1. In both cases (figure 12a, b), we have found approximately the same value for l in the passing bands. In figure 12 are also plotted two curves (1, 2) showing the frequency dependence of the viscous attenuation length of a wave propagating over a flat bottom with 1 and 2 cm water depths, which are respectively the water depths above the steps $H_0+\Delta H_1$ and $H_0+\Delta H_2$ of the bed P_1. The values of l for P_1' and P_1 are located between the limiting curves 1 and 2. We conclude from these experiments that the dissipation is not sensitive to the details of the bottom profile but depends only upon the mean characteristics of the bed.

In addition, we have visualized the vortices generated at the edge of each step. For this purpose we have deposited in pure water a small dye crystal on the top of a high

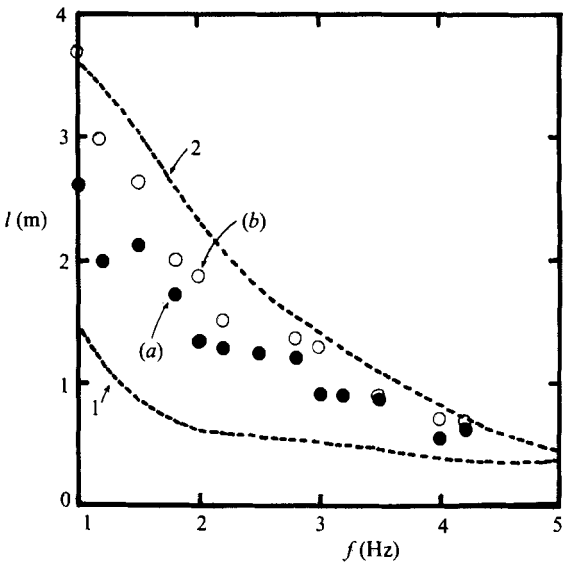

FIGURE 12. Results for the damping length l of the wave along the beds P_1 (filled circles, a) and P_1' (open circles, b) with $H_0 = 2.5$ cm, and along flat bottoms with $H_0 = 1$ cm (curve 1) and with $H = 2$ cm (curve 2).

step and observed, through the channel sidewalls, the fluid motion between this step (1) and the next lower one (2). The dye reaches the sharp corner of the step (1) on account of the drift velocity (mass transport velocity). During the wave half-cycle, when the flow is upstream, a vortex is generated at the edge of step (1) (figure 13a). During the following half-cycle when the flow reverses, a second vortex appears (figure 13b). These vortices are small features (some mm) and not symmetrical. After a complete wave cycle, a vortex pair is formed, and is then shed into the flow. The vortices appear not to be coupled between one step to the next (as compared with the case of strongly nonlinear waves with very large amplitude).

From these observations, we conclude that the contribution of vortices to dissipation in the case of the random bed R is roughly the same as for the corresponding periodic bed P: both beds possess the same number of step edges and thus the same number of uncoupled vortices, and despite the fact that the vortex strengths are greater at high steps than at low steps (for they depend upon the local amplitude of the oscillation), we may reasonably suppose that they cause the same average dissipation.

Thus, this series of auxiliary experiments has justified the assumption, already quoted in §1, that for a bed composed of steps with random height H and length L the viscous dissipation is the same as for a periodic bed having identical average characteristics, that is to say:

a step length which is the mean value of the step lengths of the random bed,

the same mean water depth H_0 as that above the random bed,

step heights alternately $H_0+\sigma_H$ and $H_0-\sigma_H$, where σ_H is the standard deviation of the step heights for the random bed, and

the same total length.

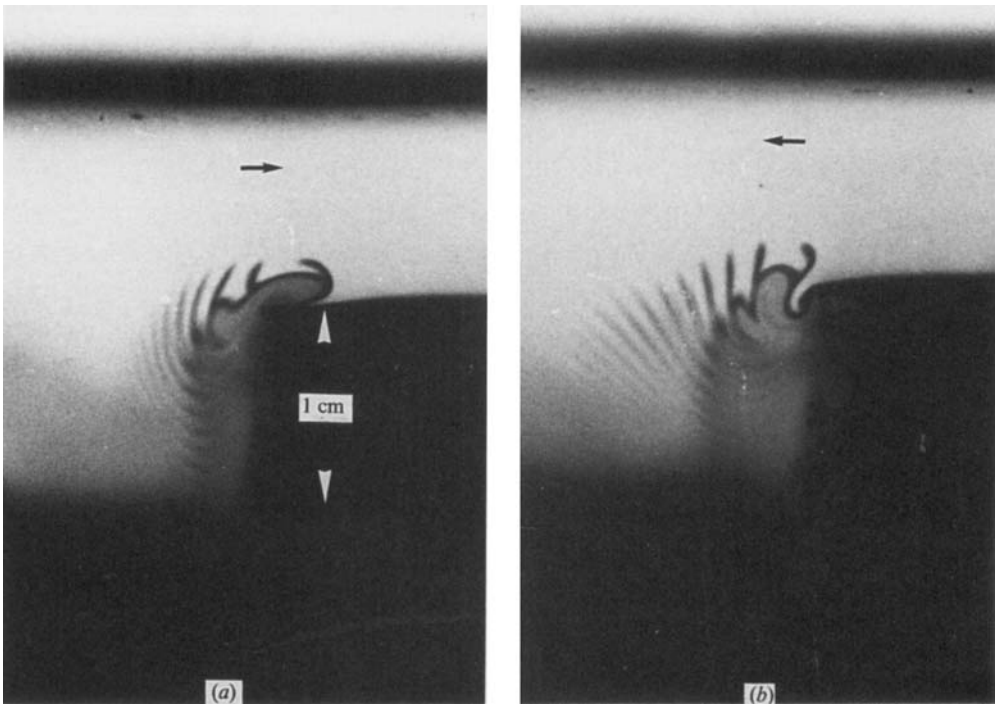

FIGURE 13. Visualization of the vortices generated at the edge of an upper step of the bed R with $H_0 = 1.75$ cm and $f = 1.9$ Hz. In (*a*) the flow is upstream and in (*b*) the flow is downstream.

3.4. *Estimation of the localization length*

The experimental values of l for the bed R are plotted on figure 14 and compared with the values obtained for the corresponding periodic bed which are, according to the above assumption, the viscous dissipation lengths d, outside the forbidden bands. For the smallest bed modulation (figure 14*a*) the disorder is not sufficient to produce a significant difference between l and d (figure 14*c*); by comparison, for the strongest disorder (figure 14*b*) the values of l in the frequency range 1–3 Hz are significantly lower (by at least 10%) than those of d (figure 14*d*). Moreover, in this latter case, $l(f)$ presents many fluctuations due to resonant modes.

Let us now extract from the total wave amplitude attenuation, characterized by the length l, the part due to the disorder, characterized by the localization length, by writing for the wave amplitude over a random bed the relation

$$A(x) \sim \exp\left(-\frac{x}{l}\right) \sim \exp\left(-\frac{x}{\xi}\right)\exp\left(-\frac{x}{d}\right), \tag{9}$$

from which a rough estimate of the localization length can be obtained:

$$\xi^{-1} = l^{-1} - d^{-1}, \tag{10}$$

where d is the viscous-attenuation length measured for the associated periodic bed, which has been extrapolated in the forbidden bands (see figure 14). This formula (10) gives an approximation for ξ when l is lower than d (at least 10% lower), in the case of a strong disorder.

The experimental estimations of the localization length are plotted in figure 15,

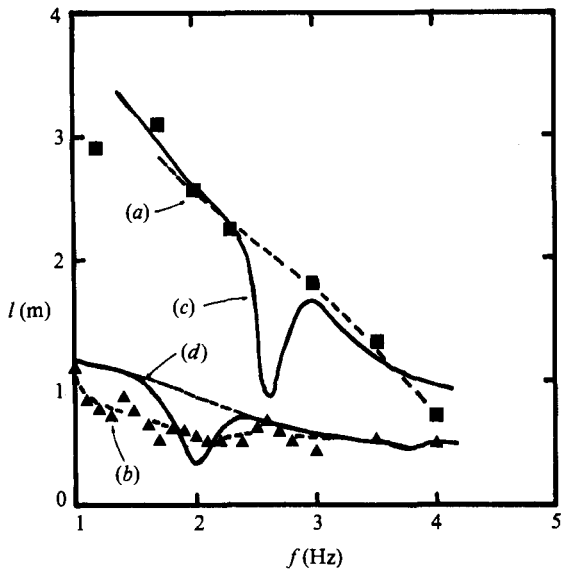

FIGURE 14. Results for the damping length l of the wave along the bed R with $H_0 = 3$ cm (curve a) and $H_0 = 1.75$ cm (curve b) and along the bed P with $H_0 = 3$ cm (curve c) and $H_0 = 1.75$ cm (curve d).

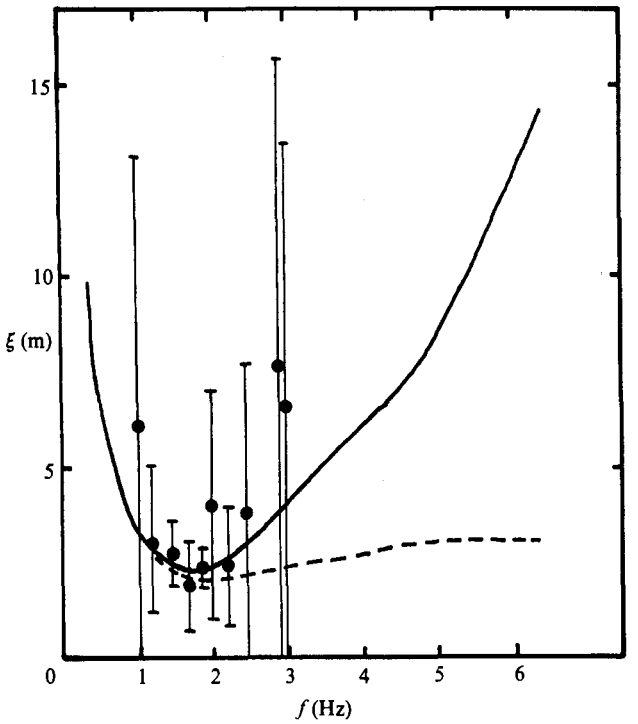

FIGURE 15. Variation of the localization length as a function of the wave frequency for the random bed R with $H_0 = 1.75$ cm ($\Delta H/H_0 = 0.71$). The dots are the experimental estimations where the average has been performed over 5 realizations of the random bed R and the full vertical lines show the standard deviations. The dotted-line and full-line curves are the numerical results of Devillard *et al.* (1987) for the shallow-water and the full potential theories, respectively.

together with the numerical calculations: more precisely, as suggested by the theory, the dots are the experimental estimations $\langle \xi^{-1} \rangle^{-1}$, where the brackets denote the average over 5 different realizations of the random bottom R composed of 58 steps; the dotted and full lines are the numerical results of Devillard *et al.* (1988) for the shallow-water and the full potential theories, respectively, in the case of the theoretical random bottom R_{th} composed of 10000 steps. In the frequency range 1.2–2.5 Hz the experimental estimations are in good agreement with the theoretical predictions of the full potential theory and moreover, one obtains the same minimal value of ξ, approximately 2 m, for the same frequency 1.7 Hz. The standard deviations shown in the figure become very important for frequencies outside the range because the localization length becomes large with respect to the size of the system and thus the experimental estimation of ξ does not have any meaning. In addition, at high frequency, viscous effects become dominant.

4. Discussion

Before the experiments described in §3 were carried out we verified that we were dealing with monochromatic linear gravity waves. Since very small wave amplitudes could be resolved with the experimental system, it was possible to confirm that typical wave steepnesses Ak were in the range 0.01–0.10, that the relative amplitude A/H was at most 0.05 and that the values of A/k^2H^3 were in the range 0.03–0.8 (the largest value corresponding to the shallow-water limit), ensuring the linearity of the waves (see (3) expressing the limitations on linear potential theory). It should be noted also that, in the frequency range of interest, the effect of surface tension was irrelevant. This was checked experimentally by verifying the dispersion relation on a flat bottom. The waves examined in the experiments reported in §3 were, thus, gravity waves in shallow water or in water of intermediate depth.

The remaining criterion involves the bed modulation $\Delta H/H_0$. Its largest value was not sufficient to induce nonlinearity in the waves. In order to identify the presence of harmonics, we examined the wave elevation as explained in §2.3 (relation (6)). This investigation revealed that more than 95% of the wave elevation was at the fundamental frequency, the remainder being in the first harmonic. This provides a clear demonstration of the linearity of the wave field.

The final criterion is that the flow above the bed should be potential. This requirement was not well satisfied since small vortices were generated at each step and shed into the flow.

The effects of these vortices as well as the friction on the bottom and the sidewalls of the tank are not taken into account in the theoretical models. The introduction of viscous effects in the computation proves rather complex, even in the case of a flat bottom: the damping lengths measured on a flat bottom are at least an order-of-magnitude smaller than those calculated by taking into account the viscous dissipation on the bottom and the sidewalls of the tank; a complete calculation should therefore take into account more complex effects (see, for example, Mei 1983, chapter 8). So we have chosen to estimate the dissipation effects experimentally. We have assumed that the dissipation for a random bottom is almost the same as for the associated periodic bottom with the same average characteristics. Various experimental checks reported in §3.3 suggested this hypothesis. We have also assumed that the total damping of the wave along the random bottom is due to a joint effect of localization and dissipation through the relation (9). This formula as well as the hypothesis about dissipation, although certainly not exact, gives a

reasonable approximation for the localization length. Nevertheless, the range of frequencies where the manifestations of the localization phenomenon could be observed was quite narrow, owing to the drastic effect of the viscosity.

Another limitation concerns the small extent of the random bottom. In the best case, namely in the frequency range 1–3 Hz, the length of the bed is of the same order as the localization length. Averages over various realizations of the random bottom have thus been taken. On the other hand, our precises experimental set-up provides a direct means of observing resonant modes (characteristics of finite-size effects) by allowing measurement of the wave amplitude all along the tank. This is the first direct experimental observation of such resonances. Moreover, it has been checked experimentally that fluctuations in wave transmission are clearly related to the occurrence of these resonances.

In other experiments on localization, resonances are seen indirectly through the fluctuations of the transmission coefficient. In addition, experiments in solid-state physics are difficult to interpret owing to additional effects of inelastic processes (such as electron–electron interaction).

5. Conclusion

Measurements of linear gravity waves on random bottoms in a one-dimensional channel give evidence of the localization phenomenon. The experimental results obtained for a random bed have been compared with those obtained for an associated periodic bed with the same average characteristics. First, it has been demonstrated that, in the case of strong disorder, the passing bands found in the periodic case have disappeared and thus the transmission is diminished. Secondly, again in the case of strong disorder, we have observed directly for the first time the resonant modes predicted by localization theory. Moreover, it has been shown that these resonant modes are directly responsible for strong fluctuations in wave transmission. Finally, in the frequency range 1.2–2.5 Hz, the damping lengths of the wave amplitude along the random bottom are lower than those obtained in the periodic case.

Since only very rough theoretical estimates of the viscous damping length can be obtained, it has been assumed, with good experimental justification, that this length is almost the same as the damping length for the associated periodic bottom. By extracting from the total wave amplitude attenuation the part due to disorder, we have estimated, in the above range of frequencies, the localization lengths. We have found good agreement between the theoretical predictions and our experimental estimations if effects associated with the finite extent of the random bed are taken into account.

It would be interesting to carry out experiments for bed geometries without sharp corners. In such cases the viscous dissipation would be reduced and the localization phenomenon would be more easily detected. Unfortunately, there are at the present time no calculations for smooth random bottoms.

We are grateful to P. Devillard, F. Dunlop and B. Souillard for numerous discussions and information about the theoretical side of this work. It is also a pleasure to thank R. Blanc, A. G. Davies and E. Guyon for many helpful discussions. We also thank B. Garceau, G. Pagni and A. Tonetto for their technical assistance. This work has been supported in part by the A.T.P. Physique Fondamentale of CNRS and by the Etablissement Public Regional Provence–Alpes–Cote d'Azur.

REFERENCES

AKKERMANS, E. & MAYNARD, R. 1984 Chains of random impedance. *J. Phys. Paris* **45**, 1549–1557.

AZBEL, M. YA, 1983 Resonance tunneling and localization spectroscopy. *Solid State Commun.* **45**, 527–530.

BALUNI, V. & WILLEMSEN, J. 1985 Transmission of acoustic waves in a random layered medium. *Phys. Rev.* **A31**, 3358–3363.

BELZONS, M., DEVILLARD, P., DUNLOP, F., GUAZZELLI, E., PARODI, O. & SOUILLARD, B. 1987 Localization of gravity waves on a rough bottom: theory and experiment. *Europhys. Lett.* (to appear).

BORLAND, R. 1963 The nature of the electronic states in disordered one-dimensional systems. *Proc. R. Soc. Lond.* A**274**, 529–545.

BOUCHAUD, E. & DAOUD, M. 1986 Reflection of light by a random layered system. *J. Phys. Paris* **47**, 1467–1475.

COHEN, S. M. & MATCHA, J. 1985 Localization of third sound by a disordered substrate. *Phys. Rev. Lett.* **54**, 2242–2245.

CONDAT, C. A. & KIRKPATRICK, T. R. 1986 Localization and resonant transmission of third-sound waves on a random substrate. *Phys. Rev.* **B33**, 3102–3114.

DALRYMPLE, R. A. & KIRBY, J. T. 1986 Water waves over ripples. *J. Waterway Port Coastal Ocean Engng Div., ASCE* **112**, 309–319.

DAVIES, A. G. 1982*a* The reflection of wave energy by undulations of the seabed. *Dyn. Atmos. Oceans* **6**, 207–232.

DAVIES, A. G. 1982*b* On the interaction between surface waves and undulations on the seabed. *J. Mar. Res.* **40**, 331–368.

DAVIES, A. G. & HEATHERSHAW, A. D. 1983 Surface wave propagation over sinusoidally varying topography: theory and observation. *Inst. Oceanogr. Sci. Rep.* 159.

DAVIES, A. G. & HEATHERSHAW, A. D. 1984 Surface-wave propagation over sinusoidally varying topography. *J. Fluid Mech.* **144**, 419–443.

DELYON, F., LÉVY, Y.-E. & SOUILLARD, B. 1985 Approach 'a la Borland' to multi-dimensional localization. *Phys. Rev. Lett.* **55**, 618–621.

DÉPOLLIER, C., KERGOMARD, X. & LALOE, F. 1986 Localisation d'Anderson des ondes dans les réseaux acoustiques unidimensionnels aléatoires. *Ann. Phys.* **11**, 457–492.

DEVILLARD, P., DUNLOP, F. & SOUILLARD, B. 1988 Localization of gravity waves on a channel with a random bottom. *J. Fluid Mech.* **186**, 521–538.

ESCANDE, D. & SOUILLARD, B. 1984 Localization of waves in a fluctating plasma. *Phys. Rev. Lett.* **52**, 1296–1299.

FLESIA, C., JOHNSTON, R. & KUNZ, H. 1987 Strong localization of classical waves: a numerical study. *Europhys. Lett.* **3**, 497–502.

GUAZZELLI, E. 1986 Deux études experimentales du désordre en hydrodynamique physique: désordre spatial de structures convectives; effet du désordre sur la propagation d'ondes de gravité. Thèse d'Etat, Université de Provence, Marseille.

GUAZZELLI, E., GUYON, E. & SOUILLARD, B. 1983 On the localization of shallow water waves by a random bottom. *J. Phys. Paris* **44**, L837–841.

HEATHERSHAW, A. D. 1982 Seabed-wave resonance and sand bar growth. *Nature* **296**, 343–345.

HEBRARD, P. & TOULOUSE, G. 1983 Etude du mouvement de la houle. *Rapport final* 2148. DERMES ONERA-CERT-Toulouse.

HODGES, C. H. 1982 Confinement of vibration by structural irregularity. *J. Sound Vib.* **82**, 411–424.

HODGES, C. H. & WOODHOUSE, J. 1983 Vibration isolation from irregularity in a nearly periodic structure: theory and measurements. *J. Acoust. Soc. Am.* **74**, 894–905.

ISHII, K. 1973 Localization of eigenstate and transport phenomena in the one-dimensional disordered system. *Prog. Theor. Phys. Suppl.* **53**, 77–138.

KITTEL, C. 1983 *Physique de l'Etat Solide*, 5ème éd. Dunod Université.

KIRBY, J. T. 1986 A general wave equation for waves over rippled beds. *J. Fluid Mech.* **162**, 171–186.

KIRKPATRICK, T. R. 1985 Localization of acoustic waves. *Phys. Rev.* **B31**, 5746–5755.

LEE, P. A. & RAMAKRISHNAN, T. V. 1985 Disordered electronic systems. *Rev. Mod. Phys.* **57**, 287–335.

MCGOLDRICK, L. F. 1968 Long waves over a wavy bottom. *University of Chicago, Department of Geophysical Sciences, ONR Ocean Science and Technology Group, Tech. Rep.* 1, 67 pp.

MEI, C. C. 1983 *The Applied Dynamics of Ocean Surface Waves.* Wiley Interscience.

MEI, C. C. 1985 Resonant reflection of surface water waves by periodic sandbars. *J. Fluid Mech.* **152**, 315–335.

MILES, J. W. 1967 Surface-wave scattering matrix for a shelf. *J. Fluid Mech.* **28**, 755–767.

MITRA, A. & GREENBERG, M. D. 1984 Slow interaction of gravity waves and a corrugated seabed. *Trans. ASME* E: *J. Appl. Mech.* **51**, 251–255.

RHINES, P. B. 1970 Wave propagation in a periodic medium with application to the ocean. *Rev. Geophys. Space Phys.* **8**, 303–319.

RHINES, P. B. & BRETHERTON, F. P. 1973 Topographic Rossby waves in a rough-bottomed ocean. *J. Fluid Mech.* **61**, 583–607.

SOUILLARD, B. 1987 Waves and electrons in inhomogeneous media. In *Chance and Matter, Proc. Les Houches* (ed. J. Souletie, J. Vannimenus & R. Stora). North-Holland.

THOULESS, D. J. 1974 Electrons in disordered systems and the theory of localization. *Phys. Rep.* **13**, 93–142.

THOULESS, D. J. 1982 Lower dimensionality and localization. *Physica* **109**, **110B**, 1523–1530.

WHITHAM, G. B. 1974 *Linear and Non Linear Waves.* Wiley.